ELSEVIER

Chemical Engineering Journal 133 (2007) 317–323

Chemical Engineering Journal

www.elsevier.com/locate/cej

The design and photoreaction kinetic modeling of a gas-phase titania foam packed bed reactor

A.O. Ibhadon [a,*], I.M. Arabatzis [b], P. Falaras [b], D. Tsoukleris [b]

[a] *Hull Environment Research Institute and Faculty of Science and the Environment, University of Hull, Cottingham Road, Hull HU6 7RX, United Kingdom*

[b] *Institute of Physical Chemistry, National Centre for Scientific Research "Demokritos", 153 10 Aghia Paraskevi Attikis, Athens, Greece*

Received 27 April 2006; received in revised form 6 February 2007; accepted 24 February 2007

Abstract

The design and testing as well as theoretical and experimental study involving kinetic modeling and photooxidation reactions of a gas-phase photocatalytic packed bed reactor (PBR) based on a porous titania foam is reported. The photoreactor was designed to incorporate a nanoporous titania foam photocatalyst for volatile organic compound (VOC) remediation in the gas-phase. Theoretical and experimental studies based on the photodegradation of model volatile organic compounds (VOCs), have been carried out and results show that 90% degradation can be achieved in the photoreactor which has been designed at low cost and to provide increased efficiency at elevated pollutant feed. The reactor represents an inexpensive design and can be applied to the remediation of various pollutants of biological, organic or inorganic origin. In addition, the reactor can accommodate the photocatalyst in the form of a thin film and porous foams.

Keywords: Modeling; Kinetics; Photocatalysis; Reactor; Titiania foam; Gas-phase

1. Introduction

Research in photocatalytic reactor design over the past two decades has concentrated on many configurations including the fixed powder layer which is illuminated from above and widely used to gather kinetic data on vapour phase photocatalytic reactions [1]; the 'transport reactor' which consists of an entrained flow of powered catalyst and examined for the partial oxidation of isobutene [2], the fluidized bed reactor which has been studied for TCE oxidation [3] and the coated monolith reactor used to study thermal catalysis in automobile exhaust converters and powder plant NO_x control installation [4].

Earlier and recent kinetic studies of vapour phase gas–solid photocatalysis exist which utilize powder layer reactors. In this configuration, a fixed photocatalyst bed is illuminated from above and passage of reactant vapour or contaminated air occurs in down-flow through the catalyst layer and supporting porous glass frit. Using data on butanol oxidation, Ollis demonstrated that this reactor configuration was free of mass transfer problems and was ideal for laboratory kinetic studies [5]. On the other hand, the partial oxidation of isobutane to acetone was explored experimentally and theoretically in a down-flow annular quartz reactor and falling titanium dioxide particles illuminated by low pressure mercury lamp. Using a set of assumptions, the reactor was modeled taking account of mass balance on acetone, the light absorption by catalyst, radial light distribution and velocity profile of the flowing gas.

The three main issues to be considered in designing a photocatalytic reactor are: (a) the analysis of the reaction (paths, mechanisms, products, efficiencies, etc.) together with the choice of the most efficient catalyst; (b) the analysis of the reaction kinetics and methods for reactor design for different reactor geometries, and (c) the provision of adequate irradiation for the whole reactor volume [6]. The first and second issues have been the subject of extensive reviews [7]. As far as the third issue is concerned, an evaluation of light absorption and development of reaction kinetic expressions that include true radiation absorption effects are needed.

Two approaches are used in analysing the results of photocatalytic reactors activated by artificial UV radiation (a) an approach based on different theoretical analysis using the radiative transfer equation and (b) an approach based on experimental

* Corresponding author. Tel.: +44 1723 357318; fax: +44 1723 370815.
E-mail address: a.o.ibhadon@hull.ac.uk (A.O. Ibhadon).

1385-8947/$ – see front matter © 2007 Elsevier B.V. All rights reserved.
doi:10.1016/j.cej.2007.02.018

Nomenclature

A_{in}	inside diameter of reactor
A_{ou}	outside diameter of reactor
C_{A_o}	reactant concentration
D	grain size
e^a	volumetric rate of radiant energy
F_{A_o}	molecular feed
k	rate constant of reaction
k_{app}	apparent first order rate constant
K	adsorption rate constant
M_o	radiation flux of reactor
M_1	radiation flux of reactor and pollutant
M_2	radiation flux of reactor, pollutant and catalyst
R	reaction rate
V	volume of reactor

Greek letters

α	constant that relates incident radiation ($m^{-2}\,s^{-1}$) to the radiation flux ($W\,m^{-2}$)
θ	surface coverage
π_a	absorbed radiation
τ	mean residence time
ϕ	fraction of light absorbed by catalyst particles
χ	conversion factor

design. Both approaches have also been extensively studied for various reactor systems including those having mass transfer limitations [8]. On the other hand, three main approaches based on experimental design in photocatalytic reactors are recognized: (i) optimal experimental design as described by Jacob et al. [9], (ii) the use of neural networks as described by Braun et al. [10] and (iii) the use of empirical approximations as proposed by Mukherjee and Ray [11]. These authors proposed the use of "reactor specific parameter" that represents the illuminated catalyst surface area in contact with reaction liquid inside the reactor volume ($m^2\,m^{-3}$) and a "reaction specific parameter" representing the average mass destruction rate ($mol\,m^{-2}\,s^{-1}$) to discuss different reactor performance.

The modeling of photoreaction kinetics usually include an evaluation of the dependence of the reaction rate on the rate of light absorption. In heterogeneous photoreactions, this cannot be measured by actinimetry. However, Yue [12], has demonstrated that this can be done by using a photodiode connected to a radiometer or photometer in the degradation of phenol in water using an annular-type immersion photoreactor and Degussa P25 photocatalyst. This method can be applied to any type of model or system and as proposed by Yue, the volumetric rate of light absorption can be determined according to Eq. (1) [12]:

$$e^a = \frac{A_{in}\phi\alpha M_o}{V} \tag{1}$$

and

$$\phi = \frac{A_{ou}(M_1 - M_2)}{A_{in}M_o} \tag{2}$$

where e^a is the local volumetric rate of energy absorption, M_o the radiation flux of reactor without the catalyst, M_1 the radiation flux of pollutant and reactor and M_2 the radiation flux of the reactor, catalyst and pollutant, A_{ou} the outside area of reactor and A_{in} the internal surface area of reactor, α a constant that relates the incident radiation (Einstein $m^{-2}\,s^{-1}$) to the radiation flux ($W\,m^{-2}$), V volume of photoreactor and ϕ is the fraction of light absorbed by the catalytic particles. A different approach was provided in a review paper [13] showed that the absorbed radiation can be calculated from

$$\pi_a = \pi_{ph}(q_i - q_t)(1 - R) \tag{3}$$

where π_{ph} is the number of photons that could be absorbed by catalyst, q_i the incident radiation, R the catalyst reflectivity and q_t is the transmitted radiation. Ollis and Turchi on the other hand [14] did not take into account light scattering, but based their proposition on Beer–Lambert equation for homogeneous systems. This work summarised the rate equations for the photocatalytic destruction of multiple water pollutants as well as simplified convective transport equations.

The work of Sclafani et al. [8] on the other hand, considered the case of photocatalytic reactors that operated under mass transport limitations. Using the oxidation of phenol by TiO_2 in a fixed bed, continuous, annular photoreactor irradiated by a high pressure mercury UV lamp as an example, they observed that the reaction rate was strongly dependent on the feed flow rate, which indicated that reactant diffusion played an important role in the process kinetics and concluded that under all experimental conditions, the reaction was controlled by mass transport. The reactor described in this work is one in which the solid phase (a nanocrystalline foam) is stationary with an immersion type' irradiation arrangement. The light source in this type of arrangement can be represented by a mathematical idealisation, a scenario that has been reviewed [12].

The aim of this study was to design a packed bed reactor incorporating a nanocrystalline foam photocatalyst for VOC remediation in the gas-phase. The reactor has many advantages over existing reactors in that the catalyst can be formed in situ in the reactor; the catalyst is contaminant non-specific and hence can be used for a wide range of pollutants and contaminants such as benzene, toluene and xylene as in this study and the separation of the catalyst from the pollutant phase as in slurry reactors is not required [15]. The reactor represents a simple and inexpensive system designed to achieve increased efficiency even at elevated pollutant feeds.

2. Experimental

2.1. Synthesis of TiO_2 foam

All chemicals and reagents used in this study were supplied by Fisher Scientific Ltd., England. Degussa P25 was kindly supplied by Degussa - AG, Germany. A viscous paste of TiO_2 is produced by mixing 2 g of Degussa P25 and the surfactant hexadecylamine (Fluka, Assay >99%) in 4 ml of boiling acetone using a molecular ratio of 1:1.5 (surfactant:TiO_2). Subsequently,

50 ml of 30% H_2O_2 is added at once. The viscous paste increases its volume to reach 150 ml of foaming material within 1 h. The titania foam is dried at ambient temperature for 2 days, before storing under vacuum at 20 mbar. The foam is the most important component of the reactor and constitutes the main novelty in this paper and as such a detailed characterization of the TiO_2 foam was undertaken using surface characterization and other techniques.

2.2. Design of a packed bed photoreactor

The real picture of the PBR is shown in Fig. 1. A cylindrical metal container with base diameter of 22 cm is used to concentrate emitted light energy from four UV-A lamps (Sylvania GTE). A Duran glass tube, diameter 1 cm and length 50 cm, is centred with its axis in parallel with the length of the cylindrical metal canister. This tube is transparent to UV light and is filled with the porous photoactive semiconductor.

The ends of the glass tube permit the inflow and outflow of the polluted gas stream. Four Sylvania F15w T8/BLBlue lamps, which have maximum emission at 350 nm of 71.7 $\mu W\,cm^{-2}$ at a distance of 25 cm, were used to provide the illumination. The lamps were placed symmetrically around the glass tube forming the outline of cross. The axis of the lamps and the glass tube are in parallel. The side distance of the lamp from the glass tube is 5 cm whilst the distance from the metal wall is 1.5 cm. The internal surface of the metal canister is coated with an adhesive aluminium foil to reflect the radiation to the glass tube housing the photocatalyst.

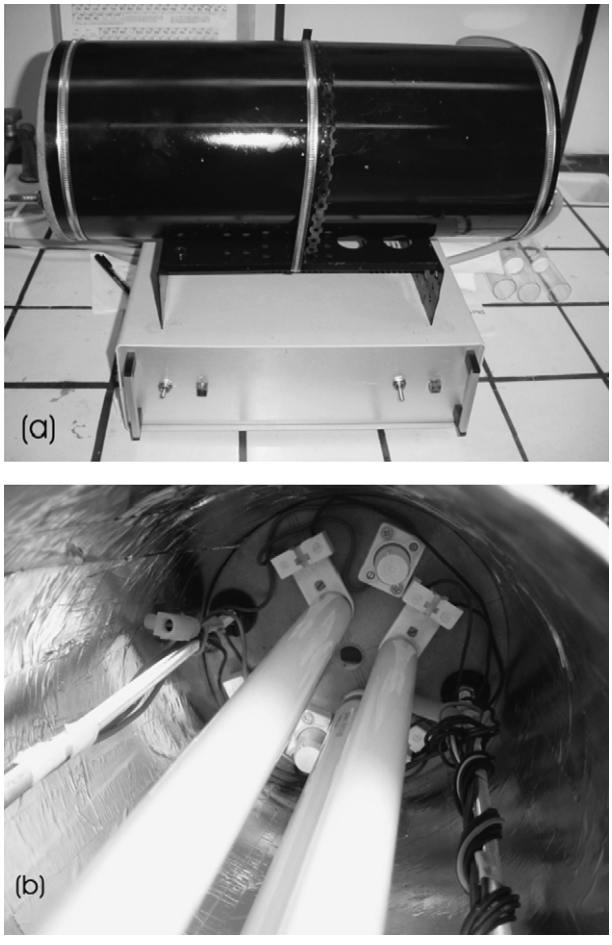

Fig. 1. The photocatalytic packed bed reactor (PPBR) used in this study: outer (a) and inner (b) views.

The PBR is closed at its ends with round wooden stops which bear the electrical set-up of the lamps (four transformers for 240 V 50 Hz ac input). The wooden stops, the lamps and the glass tube are constructed in such a way as to allow them to be inserted into and pulled out of the canister in a drawer form. This set-up ensures simple maintenance procedures and easy lamp change and hence the reactor can be deployed and operated in the batch mode or in continuous operation in a variety of reactions involving light including gas-phase photocatalysis.

2.3. Characterization of TiO_2 foam

The crystallinity of the titanium dioxide films was studied with a Siemens D-500 X-ray diffractometer (XRD, Siemens D-500, Cu Kα radiation) using Cu Kα radiation. Raman measurements were carried out with a triple Jobin-Yvon spectrometer (DILOR OMARS 89 spectrometer) equipped with a microscope and a CCD detector and a 514.5 nm argon laser. Detailed surface images were obtained by means of a scanning electron microscope (SEM) with numerical image acquisition (LEICA S440). Carbon deposition was performed to avoid problems arising from surface charge effects. X-ray from the SEM microscope probe (at horizontal incidence beam) was used for non-destructive qualitative and quantitative chemical analysis of the modified foams.

2.4. Surface properties and photocatalytic activity

The titania foams obtained are extremely rough. Their thickness was determined by an Ambios Technology (XP-2) profilometer and found to be about 20 μm. X-ray diffraction results of the titania foams Fig. 2, indicate a well organized crystal structure of titania nanoparticles. The inset picture zooms at the A(1 0 1) anatase and R(1 1 0) rutile peaks in the region of 24–28° [7]. The ratio of the two peak intensities was approximately the same (under the experimental conditions used) for the foam and Degussa P25 powder, indicating similar weight percentages of the anatase to rutile phases. The rutile content in the foam is roughly 25%, while the anatase content is about 75%. This confirms that the initial crystalline composition remained in the foam. Furthermore, the grain size was determined from the width at half maximum (w) of the A(1 0 1) anatase peak according to the Scherrer formula{8}:

$$D = \frac{0.9\lambda}{w\cos\theta} \tag{4}$$

A value of $D = 20 \pm 1$ nm was obtained for the films compared with a value of $D = 24 \pm 1$ nm obtained for Degussa P25. Difference in Scherrer value may be due to particle orientation in sample on annealing.

Raman spectroscopy is a flexible, non-destructive technique for characterization of nanostructured semiconductors. The

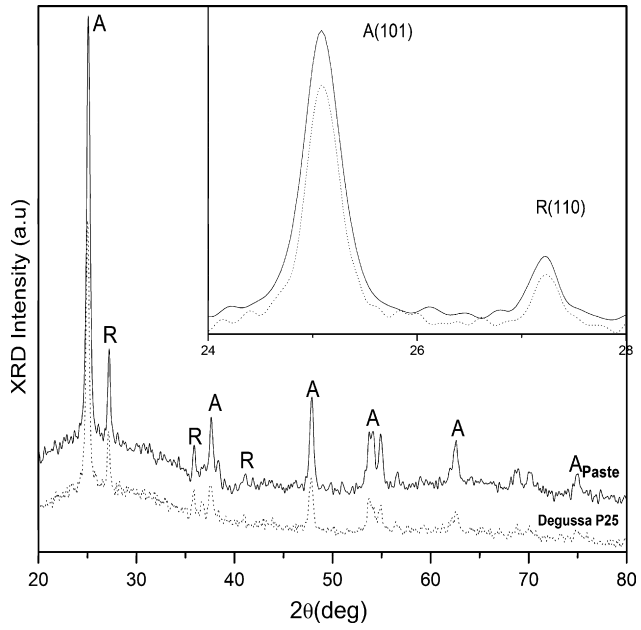

Fig. 2. X-ray diffraction image of titania foam, rutile (R) and anatase (A) phases.

technique is capable of elucidating the titania structural complexity as peaks from each crystalline phase are clearly separated in frequency, and therefore the anatase and rutile phases are easily distinguishable [9–11]. Moreover, the technique is able to detect carbonic species and evaluate the quality of thermal annealing. The Raman spectra, Fig. 3, confirm that the materials are well crystallized, without overlapped peaks and low number of imperfect sites. Vibration peaks at $142 \pm 2\,cm^{-1}$ (E_g, vs), $194 \pm 3\,cm^{-1}$ (E_g, w), $393 \pm 2\,cm^{-1}$ (B_{1g}, s), $512 \pm 1\,cm^{-1}$ (A_{1g}, s), and $634 \pm 2\,cm^{-1}$ (E_g, s) are present in the Raman spectra of the TiO_2 nanocrystalline foams, unambiguously attributed to the anatase modification. Although anatase nanoparticles are the predominant species, rutile phase is also observed as a broad peak at $446\,cm^{-1}$.

Surface morphology/characteristics is the most important factor that can affect the efficiency of a photocatalyst. Analysis performed using scanning electron microscopy (SEM), Fig. 4, revealed that the surface of the titania foam possess a sponge like

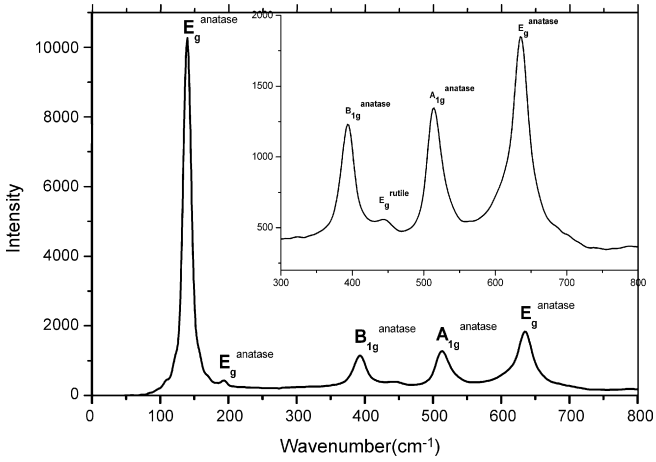

Fig. 3. Raman spectra of titania foam.

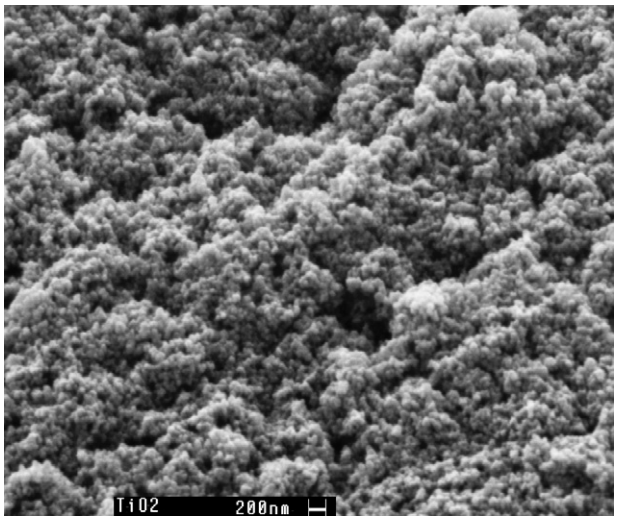

Fig. 4. Scanning microscopy image of titania foam showing highly porous architecture.

structure, with extended roughness and complex characteristics, with a particle thickness of 100 nm.

The mean diameter of the nanocrystallites is controlled by the original composition of the Degussa P25 semiconductor material. Results show that modification with an organic carrier does not induce aggregation or additional growth of the TiO_2 nanoparticles. In general, the appearance of the foam resembles a porous network with extended surface area which is ideal for heterogeneous energy conversion processes, such as the photocatalytic reactions.

2.5. Kinetic modeling

The modeling of any photocatalytic reactor includes the formation of mass balance, kinetic and radiation equations. As only kinetic modeling was carried out in this study, details of radiation equations have been omitted. For the theoretical prediction of the PBR performance, it is assumed that the porosity and structure of the photocatalyst used in this study, together with the pollutant molecular feed, permit a smooth flow of pollutant stream. For optimization needs, a molecular feed, $F_{A_o} = 10^{-4}$ mol/min is assumed with an initial pollutant concentration of $C_{A_o} = 10^{-6}$ mol/ml. The density of the ultra-light foaming semiconductor is $\rho_{bulk} = 2.93 \times 10^{-3}\,g/cm^3$. The corresponding mass of titania foam is $m_t = 10\,g$, which is the mass of foam inside the glass tube.

Theoretical results based on the above data suggest that increased photocatalytic efficiency can be obtained when the titania foam is used as a photocatalyst in the PBR. This efficiency is due to the highly porous and spongy structure of the foam. The open structure has an extended network of interconnected flakes forming irregular polygonal cavities of 200–500 nm in size, where walls with thickness of about 100 nm are visible. This structure is suitable for photocatalytic studies as the gas-phase pollutants face an extended semiconducting active surface. The crystallinity of the material as determined by means of X-ray diffraction and reported in an earlier publication [15] indicates

that the modified material mainly consists of the crystalline phase anatase whilst a 25% of the foam consists of rutile. Studies have shown that the anatase fraction of Degussa P25 is mainly responsible for the photocatalytic activity of the photocatalyst [16].

For the reactor configuration described, it has been shown experimentally that photocatalysis kinetics follow the Langmuir–Hinshelwood model [17], when the pollutant concentration is in the millimolar concentration range. This is the case because most of the toxic and mutagenic environmental contaminants are not found to exceed 10^{-4} m/l in an environmental sample. From Langmuir–Hinshelwood kinetics, the photocatalytic reaction rate, R, is proportional to the surface coverage, θ, as given in the following equation:

$$R = -\frac{dC_A}{dt} = k_r\theta = \frac{k_r K C_A}{1 + KC_A} \quad (5)$$

where k_r is the reaction rate constant, K the adsorption coefficient of the reactant and C_A is the reactant concentration. When C_A is small, $\ln(C_{A_o}/C_A) + K(C_{A_o} - C_A) = K_r Kt$, reduces to $\ln(C_{A_o}/C_A)$, and hence Eq. (5) describes a first order kinetics, the integration of which gives

$$-\ln\left(\frac{C_A}{C_{A_o}}\right) = k_{app}t \quad (6)$$

where k_{app} is the apparent first-order reaction constant. To test the effectiveness of the reactor bed, the degradation of benzene, toluene and xylene, common pollutant VOCs, was undertaken. A known concentration of VOCs mixed with air was introduced into the reactor at a flow rate of 80 μg/m^3 without (UV lamps inactive) with illumination (lamps opened) and with measurements being taken every minute using a Thermal Desorption Unit (Chrompack) coupled to a GC-FID (HP5890). The residence time of the reactants in the reactor was 8 min. Photodecomposition kinetic plots are provided in Fig. 5. The system reached equilibrium in less than 8 min by which time all of the VOCs were virtually destroyed. *o*-, *m*- and *p*-xylenes are not represented in Fig. 5, as they were completely degraded within the first 5 min of illumination.

From Eqs. (5) and (6), it is clear that the degradation of the pollutant is determined from the slow step of pollutant primary degradation. Experimental data also show that the reactor overall, actually performed better than predicted by theory. However, the percentage conversion was lower at 96.7% predicted by theory compared to 95% obtained experimentally. Experiment was carried out at ambient temperature and the system did not suffer from any pressure loss during the experiment because the gas-phase pollutants face an extended semiconducting surface due to the nanostructure of the foam as in the SEM images.

This photodegradation reaction is pseudo-first order and is understood from the following equations, which are applicable to the PBR system:

$$\text{rate limiting step :} \quad A \rightarrow B \quad (7)$$

$$\text{rate law :} \quad r = k_{app}C_A \quad (8)$$

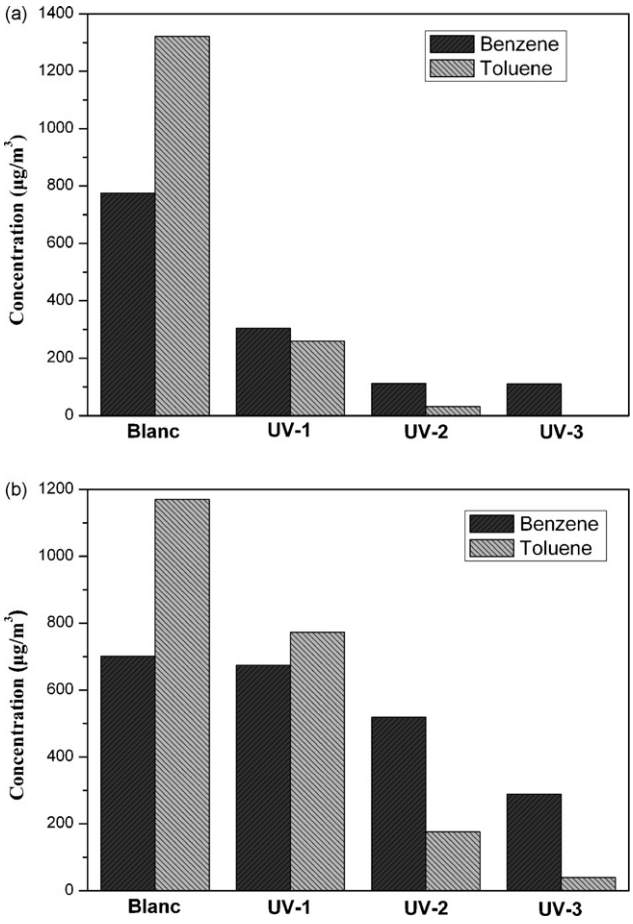

Fig. 5. Decomposition kinetics of VOC in a packed bed photoreactor: (a) four UV-A lamps and (b) two UV-A lamps.

The rate constant of most photocatalytic reactions that utilize Degussa P25 as the active material is k_{app} 0.3 min^{-1} [18]. This value of k_{app} in addition to the assumptions made are the data required to solve the following differential equations that describe the performance and efficiency of the PBR photoreactor:

the mass balance of substrate in the gas-phase is given by :

$$\frac{dx}{dW} = -\frac{r'_A}{F_{A_o}} \quad (9)$$

$$\text{rate law (kinetic equation) :} \quad -r_A = kC_A \quad (10)$$

$$\text{stoichiometry :} \quad C_A = C_{A_o}(1 - x) \quad (11)$$

where χ is the conversion factor of the pollutant. Furthermore, the mean residence time of the pollutant in the reactor is given by

$$\text{the mean residence time :} \quad \bar{\tau} = \frac{C_{A_o}V}{F_{A_o}} \quad (12)$$

$$\text{the bulk volume :} \quad V = \frac{W}{\rho_{bulk}} \quad (13)$$

The solutions to Eqs. (8)–(10) for

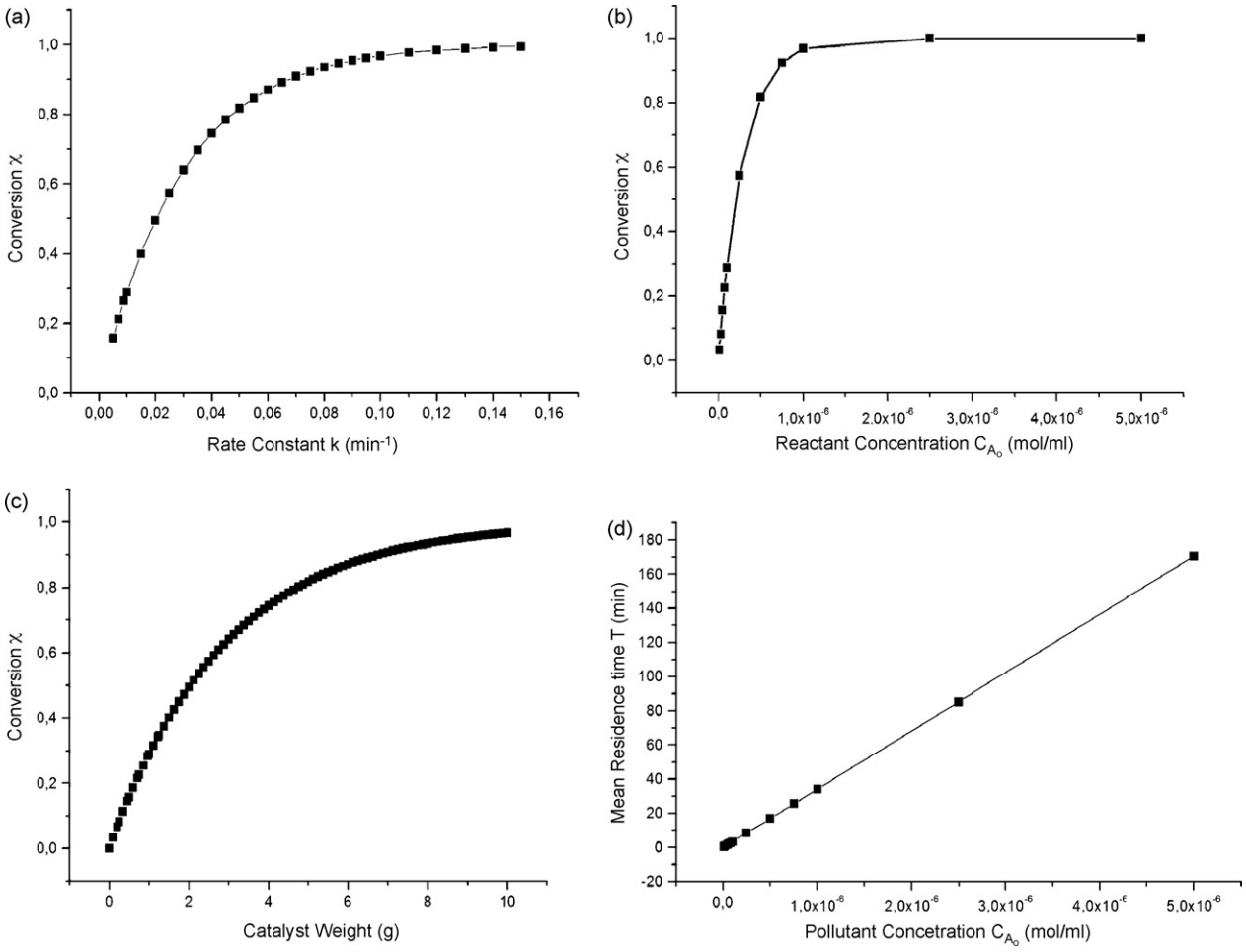

Fig. 6. (a) Conversion factor χ as a function of the rate constant, k; (b) conversion factor χ as a function of the initial pollutant concentration C_{A_o}; (c) conversion factor χ as a function of titania foam weight; (d) mean residence time τ as a function of the initial pollutant concentration C_{A_o}.

$F_{A_o} = 10^{-4}$ mol/min, $C_{A_o} = 10^{-6}$ mol/ml, $\rho_{bulk} = 2.93 \times 10^{-3}$ g/ml, $m_{kat} = 10$ g, and $k_{app} = 0.1\ min^{-1}$, yield the following values: conversion factor, $\chi = 0.967$ (96.7%) for toluene, final pollutant concentration, 3.29×10^{-6} mol/ml, mean residence time, τ, of 34.13 min. These compare well with the experimental results of $\chi = 95\%$ and τ of 10 min.

From Eqs. (8)–(10) it is possible to deduce the response of the reactor if the rate constant was varied by changing the original data. The detailed response of the system is shown in Fig. 6. From the graph of conversion against the rate constant, Fig. 6a, it is evident that for rate constants less than 0.07 min^{-1}, χ, diminishes to less than 90%. In the same way, for k_{app} values greater than 0.15 min^{-1}, the corresponding conversion almost reaches the value of 100% (99.4%).

Fig. 6b shows that the conversion, χ, increases exponentially when the pollutant concentration. The mean residence

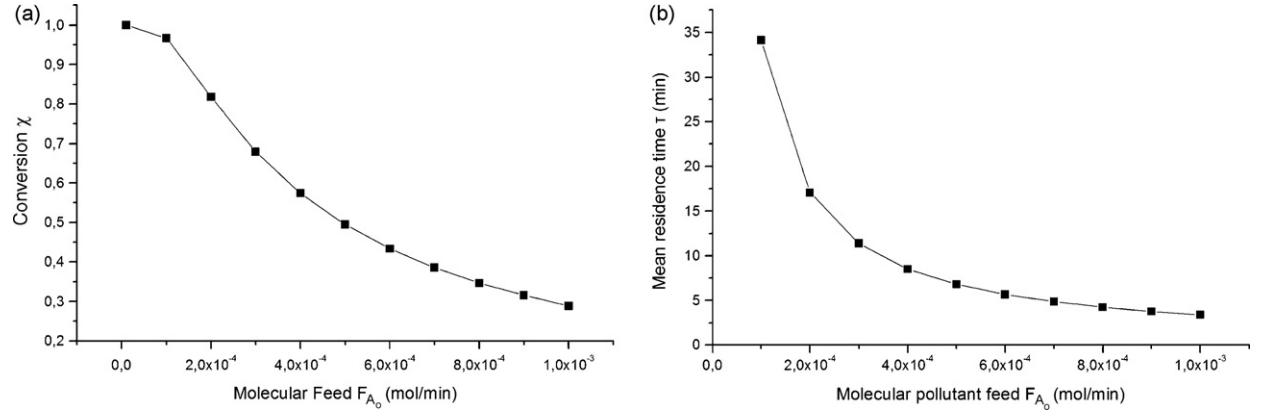

Fig. 7. (a) Conversion parameter χ as a function of molecular feed and (b) mean residence time as a function of molecular feed.

time exhibits a similar trend; although a linear increase is now obtained, Fig. 6c. These observations are expected because an increase in reactant concentration means that more molecules are found in a given photocatalyst volume. Consequently, more molecules are able to react and this increases the conversion χ. Theoretical results also indicate that concentrations below 5×10^{-7} mol/ml strongly decrease the conversion from 82% to 57%. On the other hand, for concentrations greater than 10^{-6} mol/ml, there is no significant change in the efficiency of the photoreactor. Marginal increases in catalyst load only results in a marginal increase in the conversion factor, Fig. 6d. At higher catalysts loads, problems with light scattering and insufficient absorption come into play and the magnitude of the errors in results obtained would increase with regard to the performance of the bed.

The pollutant molecular feed is an important factor with respect to the performance of the photocatalytic reactor, Fig. 7. An increase in the molecular feeding rate, F_{A_o}, leads to an exponential decay of both the conversion χ and mean residence time. An increase of the feed rate from 2×10^{-4} to 3×10^{-4} mol/min induces a decrease in the conversion χ from 81.8% to 67.9%. A further increase to 10^{-3} mol/min diminishes χ below 30%.

3. Conclusions

This study reports a theoretical study and kinetic modeling of a new packed bed photocatalytic reactor. This has been backed up by an experimental study on the degradation of benzene, toluene and xylene. The study suggests an efficient way to design and optimize a PB photocatalytic reactor. The design of the reactor is simple and economical and presents versatility with regard to the reactant type and the irradiation medium. The reactor was simulated with real initial values of the feed concentration, feed rate, catalyst and pollutant concentration and a conversion factor of 96.7% was obtained. The PBR photoreactor is a promising design for continuous flow operation with environmental samples at low and high flow rates of reactants. The illumination arrangement involving four UV lamps as well as the electrical requirement involving a transformer are easy to set-up.

Experimental data obtained on the reactor showed that the maximum conversion that could be obtained was 95%, a figure lower than theoretical predictions. It has to be borne in mind also that the titania foam may not withstand cyclic operations for a long time and the possibility that the network architecture of the pores may be affected by prolonged use exists. The reactor is efficient if low concentrations of pollutants are considered, the levels normally encountered in real environmental situations. The rate constant as well as the percentage conversion diminish considerably when pollutant concentrations exceed the millimolar range. At this concentration, increased catalyst loading only has a marginal effect, possibly due to light absorption and scattering effect problems.

Finally, the stabilization of powder consisting of nanometer-scale particles is extremely difficult both practically and experimentally. This study shows that a gas-phase reactor can be designed that exhibits the best ratio of conversion factor to reactor dimensions and photocatalyst mass. It is promising design for continuous operations involving low levels of pollutant VOCs.

Acknowledgements

The financial support from NATO (EST.CLG.979797) and GSRT/Ministry of Development-Greece, Excellence in the Research Institutes-1422/B1/3.3.1/362/2002 project and Greek–British bilateral Partnership is gratefully acknowledged. Thanks are due Dr. A.G. Kontos for Raman investigations and helpful discussions as well as to Dr. M.C. Bernard for SEM pictures and Dr. I. Raptis for thickness measurements.

References

[1] L.A. Dibble, G.B. Raupp, Kinetics of the gas–solid heterogeneous photocatalytic oxidation of trichloroethylene by near UV illuminated titanium dioxide, Catal. Lett. 4 (1990) 345.
[2] P.M. Ayoub, J. Dranoff, Proceedings of the AIChE Meeting, New York, November 1985.
[3] L. Dibble, A. Raupp, G.B. Fluidized, Bed photocatalytic oxidation of trichloroethylene in contaminated airstreams, Environ. Sci. Technol. 26 (1992) 492.
[4] K. Suzuki, S. Satoh, T. Yoshida, Photocatalytic deodorization on TiO_2 coated honeycomb ceramics, Communication 59 (6) (1991) 521.
[5] D.F. Ollis, Contaminant degradation in water, Environ. Sci. Technol. 19 (6) (1985) 480.
[6] O.M. Alfano, D. Bahnemann, A.E. Cassano, R. Dillert, R. Goslich, Photocatalysis in water environments using artificial and solar light, Catal. Today 58 (2000) 199.
[7] M.R. Hoffmann, S.T. Martin, W. Choi, D.W. Bahnemann, Environmental applications of semiconductor photocatalysis, Chem. Rev. 95 (1995) 69.
[8] A. Sclafani, A. Brucato, L. Rizzuti, in: D.F. Ollis, H. Al-Ekabi (Eds.), Photocatalytic Purification and Treatment of Water and Air, vol. 3, Elsevier, 1993, p. 533.
[9] L. Jacob, E. Oliveros, O. Legrini, A.M. Braun, in: D.F. Ollis, H. Al-Ekabi (Eds.), Photocatalytic Purification and Treatment of Water and Air, vol. 3, Elsevier, 1993, p. 511.
[10] A.M. Braun, L. Jacob, E. Oliveros, Oller do Nacimento, Up-scaling photochemical reactions, Adv. Photochem. 18 (1993) 235.
[11] P.S. Mukherjee, A.K. Ray, Major challenges in the design of large scale photocatalytic reactor for water treatment, Chem. Eng. Technol. 22 (3) (1999) 253.
[12] P.L. Yue, in: D.F. Ollis, H. Al-Ekabi (Eds.), Milne in Photocatalytic Purification and Treatment of Water and Air, vol. 3, Elsevier, 1993, p. 495.
[13] N. Serpone, G. Sauve, R. Koch, H. Tahiri, P. Pichat, E. Pelizzetti, H. Hidaka, J. Photochem. Photobiol. A: Chem. 94 (1996) 191–203.
[14] D. Ollis, F.C. Turchi, Heterogeneous photocatalysis for water purification: contaminant mineralisation kinetics and elementary reactor analysis, Environ. Prog. 9 (4) (1990) 229.
[15] I.M. Arabatzis, P. Falaras, Synthesis of porous nanocrystalline titanium dioxide foam, Nanoletters 3 (2) (2003) 249.
[16] V.A. Sakkas, I.M. Arabatzis, I.K. Konstantinou, A.D. Dimou, T.A. Albanis, P. Falaras, Appl. Catal. B: Environ. 49 (2004) 195–205.
[17] H. Al-Ekabi, N. Serpone, Kinetic studies in heterogeneous photocatalysis. Photocatalytic degradation of chlorinated phenols in aerated aqueous solutions over TiO_2 supported on a glass matrix, J. Phys. Chem. 92 (1988) 5726.
[18] I.M. Arabatzis, T. Stergiopoulos, D. Andreeva, S. Kitova, S.G. Neophytides, P. Falaras, J. Catal. 220 (2003) 127–135.